Isoprene photochemistry over the Amazon rainforest

Yingjun Liu[a], Joel Brito[b], Matthew R. Dorris[c], Jean C. Rivera-Rios[c,d], Roger Seco[e], Kelvin H. Bates[f], Paulo Artaxo[b], Sergio Duvoisin Jr.[g], Frank N. Keutsch[a,c,d], Saewung Kim[e], Allen H. Goldstein[h], Alex B. Guenther[e,i], Antonio O. Manzi[j], Rodrigo A. F. Souza[k], Stephen R. Springston[l], Thomas B. Watson[l], Karena A. McKinney[a,1], and Scot T. Martin[a,m,1]

[a]John A. Paulson School of Engineering and Applied Sciences, Harvard University, Cambridge, MA 02138; [b]Department of Applied Physics, University of São Paulo, São Paulo 05508, Brazil; [c]Department of Chemistry, University of Wisconsin-Madison, Madison, WI 53706; [d]Department of Chemistry and Chemical Biology, Harvard University, Cambridge, MA 02138; [e]Department of Earth System Science, University of California, Irvine, CA 92697; [f]Division of Chemistry and Chemical Engineering, California Institute of Technology, Pasadena, CA 91125; [g]Department of Chemistry, Universidade do Estado do Amazonas, Manaus, AM 69050, Brazil; [h]Department of Environmental Science, Policy, and Management, University of California, Berkeley, CA 94720; [i]Pacific Northwest National Laboratory, Richland, WA 99354; [j]Instituto Nacional de Pesquisas da Amazonia, Manaus, AM 69067, Brazil; [k]Department of Meteorology, Universidade do Estado do Amazonas, Manaus, AM 69050, Brazil; [l]Department of Environmental and Climate Sciences, Brookhaven National Laboratory, Upton, NY 11973; and [m]Department of Earth and Planetary Sciences, Harvard University, Cambridge, MA 02138

Edited by Mark H. Thiemens, University of California, San Diego, La Jolla, CA, and approved April 13, 2016 (received for review December 23, 2015)

Isoprene photooxidation is a major driver of atmospheric chemistry over forested regions. Isoprene reacts with hydroxyl radicals (OH) and molecular oxygen to produce isoprene peroxy radicals (ISOPOO). These radicals can react with hydroperoxyl radicals (HO_2) to dominantly produce hydroxyhydroperoxides (ISOPOOH). They can also react with nitric oxide (NO) to largely produce methyl vinyl ketone (MVK) and methacrolein (MACR). Unimolecular isomerization and bimolecular reactions with organic peroxy radicals are also possible. There is uncertainty about the relative importance of each of these pathways in the atmosphere and possible changes because of anthropogenic pollution. Herein, measurements of ISOPOOH and MVK + MACR concentrations are reported over the central region of the Amazon basin during the wet season. The research site, downwind of an urban region, intercepted both background and polluted air masses during the GoAmazon2014/5 Experiment. Under background conditions, the confidence interval for the ratio of the ISOPOOH concentration to that of MVK + MACR spanned 0.4–0.6. This result implies a ratio of the reaction rate of ISOPOO with HO_2 to that with NO of approximately unity. A value of unity is significantly smaller than simulated at present by global chemical transport models for this important, nominally low-NO, forested region of Earth. Under polluted conditions, when the concentrations of reactive nitrogen compounds were high (>1 ppb), ISOPOOH concentrations dropped below the instrumental detection limit (<60 ppt). This abrupt shift in isoprene photooxidation, sparked by human activities, speaks to ongoing and possible future changes in the photochemistry active over the Amazon rainforest.

isoprene photochemistry | Amazon | organic hydroperoxides

Isoprene (C_5H_8) accounts for approximately half of the global flux of nonmethane biogenic volatile organic compounds to the atmosphere (1). The reactive chemistry of isoprene influences the oxidative capacity of the troposphere and the associated chemical cycles of atmospheric trace gases (2, 3). Isoprene photooxidation products are also important sources of atmospheric organic particulate matter (4–6). Isoprene is mostly oxidized in the atmospheric mixed layer, although entrainment and reaction in the free troposphere can also be important (7, 8).

Isoprene oxidation is mostly initiated by an addition reaction of a photochemically produced hydroxyl radical (OH) across the double bond, followed by the rapid addition of molecular oxygen (O_2) to the primary radical. A population of isoprene peroxyl radicals (ISOPOO) is thereby produced. The subsequent chemistry of ISOPOO radicals proceeds along several competing pathways (9). Reaction of ISOPOO with nitric oxide (NO) dominates in polluted regions of the planet. The major products are methyl vinyl ketone (MVK, C_4H_6O) and methacrolein (MACR, C_4H_6O).

The fate of ISOPOO radicals over unpolluted regions of the planet remains unclear. For many isoprene source regions, reaction of ISOPOO with hydroperoxyl radicals (HO_2) has been taken as the dominant pathway (5, 10–13), including over remote tropical forests like Amazonia where there are few anthropogenic NO sources. The major products of the HO_2 pathway are an isomeric family of hydroxyl hydroperoxides (ISOPOOH; $C_5H_{10}O_3$). In addition, isomerization and bimolecular reactions with other organic peroxyl radicals (RO_2) can also be important (10, 14, 15). Measurements of HO_2, RO_2, and NO, if available, could help to constrain these pathways for unpolluted regions, but each of these measurements is challenging in its own way (16, 17), and available data sets are sparse (2, 18). Unimolecular ISOPOO isomerization, for its part, remains in the early stages of study (10, 15). As a result, the relative contribution of each pathway to the fate of atmospheric ISOPOO radicals remains uncertain for unpolluted regions of Earth (19).

The uncertainty in ISOPOO reaction pathways, in particular the uncertainties of the contributions of NO and HO_2 pathways, hinders accurate prediction of the environmental and climate impacts of isoprene chemistry. The HO_2 reaction pathway is important for the production of particulate matter through second-generation epoxydiol products (5, 6). The NO pathway contributes to the transport of nitrogen beyond the isoprene source region through the formation of stable organic nitrogen compounds (20). The two pathways, to different extents, help to maintain the atmospheric oxidation cycle, including feedbacks on OH and O_3 concentrations (3, 5, 11).

Accurate ambient measurements of the molecular identities and concentrations of isoprene oxidation products are a first-order

Significance

For isolated regions of the planet, organic peroxy radicals produced as intermediates of atmospheric photochemistry have been expected to follow HO_2 rather than NO pathways. Observational evidence, however, has been lacking. An accurate understanding of the relative roles of the two pathways is needed for quantitative predictions of the concentrations of particulate matter, oxidation capacity, and consequent environmental and climate impacts. The results herein, based on measurements, find that the ratio of the reaction rate of isoprene peroxy radicals with HO_2 to that with NO is about unity for background conditions of Amazonia. The implication is that sufficient NO emissions are maintained by natural processes of the forest such that both HO_2 and NO pathways are important, even in this nominally low-NO region.

Author contributions: Y.L., P.A., F.N.K., A.H.G., A.B.G., A.O.M., R.A.F.S., K.A.M., and S.T.M. designed the research; Y.L., J.B., M.R.D., J.C.R., R.S., K.H.B., S.D., S.K., S.R.S., and T.B.W. performed the research; Y.L., K.A.M., and S.T.M. analyzed the data; and Y.L., K.A.M., and S.T.M. wrote the paper.

The authors declare no conflict of interest.

This article is a PNAS Direct Submission.

[1]To whom correspondence may be addressed. Email: kamckinney@seas.harvard.edu or scot_martin@harvard.edu.

This article contains supporting information online at www.pnas.org/lookup/suppl/doi:10.1073/pnas.1524136113/-/DCSupplemental.

requirement for testing concepts of the reaction pathways of isoprene and the associated predictions of chemical transport models (CTMs). The products MVK and MACR have been studied in many atmospheric environments both by proton transfer reaction mass spectrometry (PTR-MS) and gas chromatography (GC) (21). Large data sets are available (7, 8, 21, 22). By comparison, ambient measurements of ISOPOOH isomers are sparse, and available data sets are limited to temperate regions (23, 24).

An additional issue is that the utility of existing data sets of MVK and MACR concentrations to test and constrain models of isoprene chemistry is challenged by recent laboratory studies that have shown that both PTR-MS and GC techniques can have a contribution from ISOPOOH species in the nominal detection of MVK and MACR (11, 13). For the usual operating conditions of PTR-MS and GC instrumentation, the two main ISOPOOH isomers [specifically, (1-OH, 2-OOH)-ISOPOOH, hereafter (1, 2)-ISOPOOH, and (4-OH, 3-OOH)-ISOPOOH, hereafter (4, 3)-ISOPOOH] decompose on the hot metal surfaces inside both types of instruments (13). The (1, 2)-ISOPOOH and (4, 3)-ISOPOOH decompose to MVK and MACR, respectively. In this case, MVK and MACR concentrations reported in the literature can be expected to be upper limits, rather than best estimates, for regions of Earth where the HO_2 pathway is important for the fate of ISOPOO radicals. On a planetary scale, the contribution of the HO_2 pathway has been modeled as 60% larger than that of the NO pathway (10). The need for corrections to MVK and MACR data sets could be widespread.

In light of these issues, the present study was undertaken to measure the sum of (1, 2)-ISOPOOH and (4, 3)-ISOPOOH concentrations (hereafter, ISOPOOH concentration), in comparison with the sum of MVK and MACR concentrations. The measurements took place in the central region of the Amazon basin during the wet season of 2014. The measurements were made as part of the Observations and Modeling of the Green Ocean Amazon (GoAmazon2014/5) experiment (25). A major concept of the experiment was to locate a research site (T3) several hours downwind of an urban region (specifically, 70 km west of Manaus, Amazonas, Brazil, a city of 2 million people). Local winds at different times swept either the pollution plume of Manaus or background air of the Amazon basin across the research site. As a result, the species observed at T3 were at times produced upwind under background conditions whereas, at other times, they were significantly affected by pollution. Based on back-trajectories, the most probable transport time from the city to the measurement site was between 4 h and 5 h. By comparison, (4, 3)-ISOPOOH, isoprene, (1, 2)-ISOPOOH, MACR, and MVK have characteristic lifetimes to OH loss of ~2 h, 3 h, 4 h, 10 h, and 14 h, respectively, for a reference OH concentration of 10^6 cm^{-3} typical of many environments. Deposition and entrainment can also be important loss mechanisms (26, 27). Background air, meaning the Amazon basin in the nominal absence of the pollution plume of Manaus, had significant variability associated with it, especially with respect to effective photochemical age. Background variability arose from variations of in-basin emissions and transformations integrated across several days of meteorology as well as, at times, from significant out-of-basin influences and variability tied to transport from the Atlantic Ocean and Africa (28, 29). Even so, the effect of the plume, when present, dominated over this background variability for the measured quantities of the present study. Measurements of the ratio of ISOPOOH to MVK + MACR concentrations, reported herein, are used to assess how different amounts of pollution, including background conditions in the absence of anthropogenic influence (i.e., low NO), regulate the relative importance of isoprene photooxidation pathways in the tropical forest of central Amazonia.

Observations

Data sets were collected at the T3 site of GoAmazon2014/5 in the wet season during an 8-week intensive operating period (*SI Appendix*). Concentrations of ISOPOOH and MVK + MACR were measured using a proton transfer reaction time-of-flight mass spectrometer (PTR-TOF-MS). ISOPOOH and MVK + MACR, both detected as the $C_4H_7O^+$ ion by the PTR-TOF-MS, were discriminated by use of an upstream cold trap. ISOPOOH, having a lower volatility than does MVK or MACR, was selectively removed by the cold trap (11, 30).

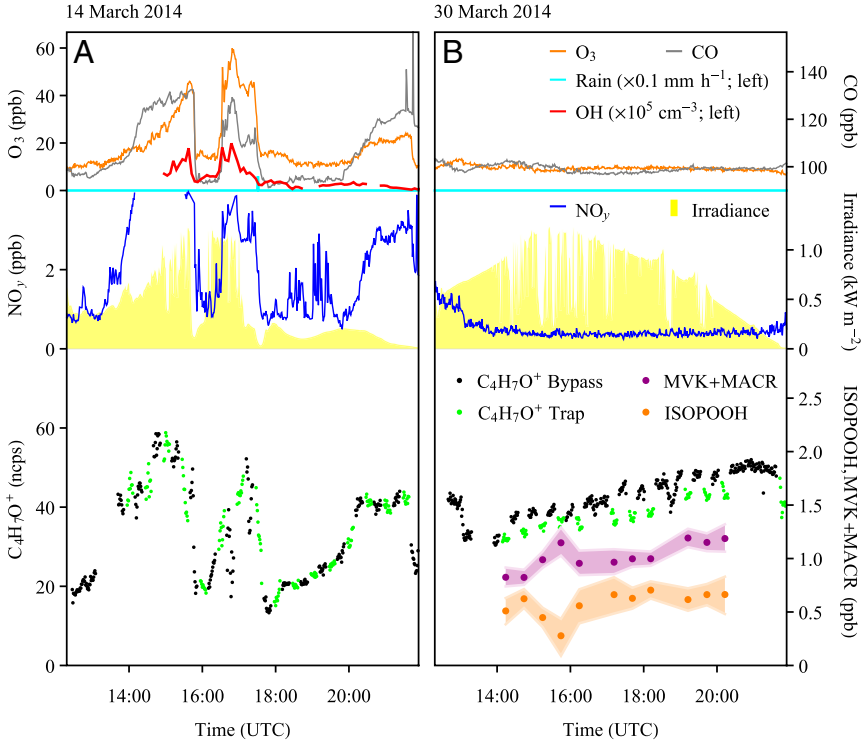

Fig. 1. Representative afternoon time series of (*Top*) CO concentrations, O_3 concentrations, OH concentrations, and rain amount; (*Middle*) NO_y concentrations and shortwave broadband total down-welling irradiance; and (*Bottom*) signal intensities of $C_4H_7O^+$ ions and concentrations of MVK+MACR and ISOPOOH. Lifetimes of CO, O_3, and OH are many days, many hours, and less than 1 s, respectively, over the tropical forest in Amazonia. (*A*) Polluted conditions (14 March 2014). The weather was partly cloudy with scattered showers. (*B*) Background conditions (30 March 2014). The weather was sunny, and there was no rainfall. Local noon is at 1600 UTC. The green and black points for the $C_4H_7O^+$ ions represent intensities with and without the cold trap in place, respectively. Intensities are given in normalized counts per second (ncps) (*SI Appendix*). For concentrations of MVK + MACR and ISOPOOH, the light shadings represent 75% confidence intervals. Measurements of OH concentrations are not available for 30 March 2014.

Fig. 1 shows the time series of trap and bypass signal intensities of the $C_4H_7O^+$ ion for two contrasting afternoons. The time series of the concentrations of reactive nitrogen compounds (NO_y), ozone (O_3), and carbon monoxide (CO) show that Fig. 1 *A* and *B* correspond, respectively, to time periods when the pollution plume or background air passed over T3. The NO_y concentration is defined as the sum concentration of NO, NO_2, and compounds produced from them. NO_y favors NO and NO_2 near source regions and remains a semiconserved quantity downwind as NO and NO_2 are incorporated into product molecules. The instantaneous concentrations of NO at T3 are often below detection limit [70 parts per trillion (ppt)] because of the rapid titration of this species by peroxy radicals and ozone, even as it remains an important reactant. For these reasons, NO_y concentration is used in this study as a surrogate variable for the integrated effects of NO on the chemistry that took place during transport to T3. As a reference point, background air in the boundary layer of the central Amazon basin in the wet season is characterized by 0.5 ± 0.3 parts per billion (ppb) of NO_y (31).

On the afternoon affected by pollution, the NO_y concentrations measured at T3 were regularly above 1 ppb (Fig. 1*A*, *Middle*). The concentrations of O_3 and CO were also elevated (Fig. 1*A*, *Top*). Back-trajectories from T3 show that the air came from Manaus (*SI Appendix*, Fig. S1*A*). Under the influence of this pollution, the trap and bypass intensities for the $C_4H_7O^+$ ion followed each other closely (Fig. 1*A*, *Bottom*), without any statistically significant differences. The conclusions for this polluted afternoon are that the NO pathway dominated over the HO_2 pathway for the fate of ISOPOO radicals and that the $C_4H_7O^+$ intensity predominantly arose from MVK and MACR, without any contribution by ISOPOOH.

Fluctuations are apparent in the data sets of Fig. 1*A* at several time points throughout the day. The fluctuations at 1600 UTC arose from a 45-min shift in the local winds from polluted easterlies to background southerlies associated with a local convective cell (*SI Appendix*, Fig. S2). Atmospheric concentrations of the measured species decreased because of a combination of wet deposition and convective mixing with clean air. The precipitous drops in the data sets at 1745 UTC were associated with rainfall. At other times, small fluctuations reflected variations in the amounts of Manaus pollution that reached the measurement site during the course of the observations. The $C_4H_7O^+$ intensity fluctuated in correlation with the NO_y concentration (Fig. 1*A*, *Middle* compared with *Bottom*). MVK and MACR were produced more rapidly in air masses having higher NO_y concentrations because the atmospheric oxidation cycle was accelerated (32). As an example of this acceleration, the instantaneous OH concentration increased markedly when pollution and sunlight were simultaneously present (Fig. 1*A*, *Top*).

During the afternoon of background conditions, the NO_y concentration at T3 varied little from 0.4 ppb throughout the day (Fig. 1*B*, *Middle*). Ozone and carbon monoxide had concentrations typical of background air masses in the wet season (Fig. 1*B*, *Top*) (29). Back-trajectories launched from T3 showed that the air did not intersect Manaus. The air instead came from remote regions of the Amazon basin (*SI Appendix*, Fig. S1*B*). Under these conditions, the HO_2 pathway played an important role in the fate of ISOPOO radicals, and, on this afternoon, the $C_4H_7O^+$ intensity with the cold trap in place was lower than in its absence (Fig. 1*B*, *Bottom*).

A difference signal $\Delta C_4H_7O^+$ measured with and without the trap can be defined (*SI Appendix*). A nonzero $\Delta C_4H_7O^+$ is attributed to the presence of ISOPOOH (11). The possibility of significant contributions by other compounds to $\Delta C_4H_7O^+$, such as pinonaldehyde and isoprene epoxydiols (IEPOX) (30), was considered but ruled out (*SI Appendix*). The difference signal $\Delta C_4H_7O^+$ was converted to ISOPOOH concentration based on calibrations using synthesized standards of ISOPOOH isomers. The MVK+MACR concentration was subsequently determined. For the afternoon of background conditions, the ISOPOOH concentration was ~0.6 ppb throughout the day (Fig. 1*B*, *Bottom*). The MVK + MACR concentration increased from 0.9 ppb to 1.2 ppb. For comparison, daytime ISOPOOH concentrations in the western United States of up to 1 ppb were reported using CF_3O^- as the ionization agent in a chemical ionization mass spectrometer, although authentic standards were not available for instrument calibration (23). A similar instrument, but with calibration, subsequently measured 0.4 ppb as the daytime ISOPOOH + IEPOX concentration in the southeastern United States (24).

Twenty-three days of daytime trap data were obtained during the measurement period, and a statistical analysis was carried out (Fig. 2). The $\Delta C_4H_7O^+$ values were grouped by NO_y concentration such that each of the six data subsets had an equal number of data points. Quartile and median values of $\Delta C_4H_7O^+$ intensity and NO_y concentration were calculated for each subset. Results are plotted in Fig. 2*A*. For subsets of NO_y > 1 ppb, indicating the influence of the Manaus pollution plume, the medians were approximately zero (Fig. 2*A*), meaning that no ISOPOOH was detected for these conditions. By comparison, for subsets having NO_y < 1 ppb, indicating the sampling of background air, the medians increased for decreasing NO_y concentration. The implication is that ISOPOOH concentrations increased with lower NO_y concentrations.

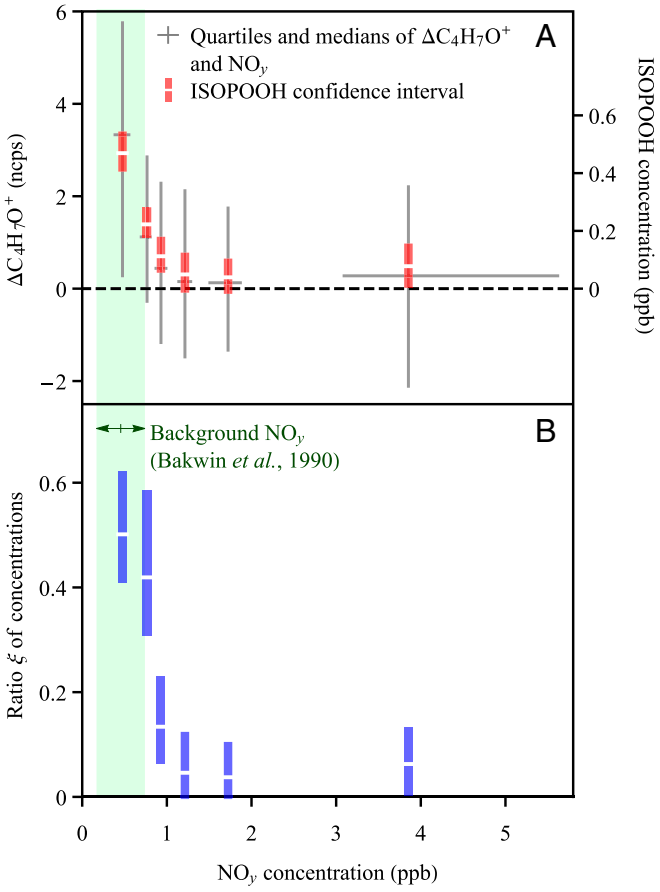

Fig. 2. Dependence of observations on NO_y concentration. (*A*) Quartiles and median of $\Delta C_4H_7O^+$ measurements. The central value of the ISOPOOH concentration, corresponding to the median of the $\Delta C_4H_7O^+$ measurements, is also shown. The bar represents the 75% confidence interval around the central value of the obtained ISOPOOH concentration. (*B*) Ratio ξ of ISOPOOH concentration to that of MVK + MACR. The central value of the ratio is based on the median of the $\Delta C_4H_7O^+$ measurements. The bar represents the 75% confidence interval around the central value of the obtained ratio. Light green shading represents NO_y concentrations of background air masses in the central Amazon basin in the wet season (31).

The central values of the ISOPOOH concentrations derived from the median values of the $\Delta C_4H_7O^+$ measurements are represented on the right axis of Fig. 2*A*. The bar represents the 75% confidence interval around the central value of the obtained ISOPOOH concentration. Medians of $\Delta C_4H_7O^+$ (left axis) and central values of ISOPOOH concentrations (right axis) are slightly offset from one another because of nonlinearity in the ISOPOOH calibration, including a dependence on humidity (*SI Appendix*). For the bin of lowest NO_y concentration, which corresponds to 0.5 ppb as a median value, the central value of the ISOPOOH concentration was 0.5 ppb. This NO_y bin is coincident with the envelope of 0.5 ± 0.3 ppb characteristic of background conditions in the wet season of Amazonia (31).

The concentration of ISOPOOH compared with that of MVK + MACR, represented as a ratio quantity ξ, was calculated, and its relationship to NO_y was analyzed. Fig. 2*B* plots the central value of ξ and its 75% confidence interval (bar length) for each NO_y bin. The ratio ξ decreases for increasing NO_y concentration, approaching zero for $NO_y > 1$ ppb. For the lowest NO_y concentration, characteristic of background conditions, the central value of ξ was 0.5 (0.4–0.6 with uncertainty).

From a technical perspective, ξ can indicate the possible quantitative error in the historical assumption that the $C_4H_7O^+$ signal arose exclusively from MVK and MACR. Fig. 2*B* shows that ξ changed with NO_y concentration for $NO_y < 1$ ppb but was close to zero for $NO_y > 1$ ppb. A criterion of $NO_y > 1$ ppb is, therefore, suggested as a simple heuristic check before attributing the $C_4H_7O^+$ signal in future studies exclusively to MVK and MACR concentrations. This heuristic applies assuming that the dependence observed in the wet season of the central Amazon basin also applies to other environments. More generally, a confidence interval of 0.4–0.6 for ξ under background conditions in central Amazonia suggests that the nominal MVK and MACR concentrations reported in the literature for remote locations are in need of correction for ISOPOOH contributions when PTR-MS, GC, or other methods having hot metal surfaces were used for the measurements.

Modeling

The observed concentration ratio ξ can be used in an analytical model to estimate the ratio χ of the production rate of ISOPOOH to that of MVK + MACR. This ratio corresponds to $(S_1 + S_2)/(S_3 + S_4)$ for production rates S_i (molec cm^{-3} s^{-1}) of species i. Species 1–4 correspond to (1, 2)-ISOPOOH, (4, 3)-ISOPOOH, MVK, and MACR, respectively. Quantities ξ and χ differ from one another because of the different atmospheric lifetimes of species i. For initial concentrations of zero and for production rates S_i and loss coefficients k_i (s^{-1}) that are constant, the following result can be obtained to relate χ to ξ for a reaction time t (*SI Appendix*):

$$\chi = \frac{(0.6/k_3)\left(1-e^{-k_3 t}\right) + (0.4/k_4)\left(1-e^{-k_4 t}\right)}{(0.6/k_1)(1-e^{-k_1 t}) + (0.4/k_2)(1-e^{-k_2 t})}\xi. \qquad [1]$$

Composite, pseudo–first-order loss coefficients k_i are given by $k_i = k_{i,\mathrm{OH}}[\mathrm{OH}] + k_{i,en} + k_{i,d}$ for bimolecular reactions with OH, atmospheric entrainment (*en*), and surface deposition (*d*). On-site measurements of OH concentrations by chemical ionization mass spectrometry (33), recent advances in the understanding of the deposition processes of ISOPOOH (26), and an approximate description of the boundary layer dynamics over the Amazonia (34) allow reasonable estimates of the loss coefficients k_i (*SI Appendix*, Table S1).

The model derivation relies on the accuracy of two approximations. (*i*) Species concentrations are taken as zero at sunrise, which then represents time zero. This approximation is well supported by measured concentrations, which at sunrise were <5% of the maximum measured daily concentrations (*SI Appendix*, Fig. S3). (*ii*) Production rates S_i and loss coefficients k_i are approximated as constant throughout the day, thereby corresponding to average or effective daily values. The sensitivity of the results to this approximation is examined in *SI Appendix*.

Eq. **1** shows that the production ratio χ is proportional to the concentration ratio ξ for any fixed reaction time. For an average daytime OH concentration of 5×10^5 cm^{-3} for background conditions (33) and an effective reaction time of 5 h representing daybreak to midafternoon, the proportionality coefficient is 1.5 (*SI Appendix*, Fig. S4). The confidence interval of 0.4–0.6 for ξ under background conditions (Fig. 2*B*) implies a range of 0.6–0.9 for χ. The appropriateness of the effective photochemical reaction time (i.e., 5×10^5 OH cm^{-3} for 5 h) is verified by the agreement of the predicted and measured ratios given by the total concentration of reaction products (i.e., sum of MVK, MACR, and ISOPOOH) divided by the isoprene concentration (*SI Appendix*).

The product-focused methodology to determine χ can be complemented by a source-based analysis. Reactions of ISOPOO serve as the sources of ISOPOOH and MVK + MACR. In a source-based analysis, the production ratio χ is expressed as follows:

$$\chi = \frac{Y_{\mathrm{ISOPOOH,\,HO_2}} f_{\mathrm{HO_2}}}{\sum_{j\in\{\mathrm{HO_2,NO,RO_2,ISOM}\}} Y_{\mathrm{MVK+MACR},\,j}\, f_j} \qquad [2]$$

The fractional yield of ISOPOOH in the reaction of ISOPOO with HO_2 is represented by the term $Y_{\mathrm{ISOPOOH,HO_2}}$, which has an estimated value of 0.90 (35). By comparison, ISOPOOH is believed to be produced neither from the reactions of ISOPOO with NO and RO_2 nor by isomerization. The fraction yield of MVK + MACR in pathway j of the ISOPOO reaction is represented by the term $Y_{\mathrm{MVK+MACR},\,j}$. The best-estimate values for NO, HO_2, RO_2 and isomerization (ISOM) pathways are 0.06, 0.71, 0.75, and 0.10, respectively (*SI Appendix*, Table S2 and references therein).

Term f_j of Eq. **2** is the fractional contribution of pathway j to ISOPOO loss. The fractions of the NO, HO_2, RO_2, and isomerization pathways sum to unity. These fractions were obtained for NO concentrations ranging from background to polluted conditions using a box model based on the Master Chemical Mechanism (version 3.3.1) and supplemented by recent experimental results (9, 11, 35). For straightforwardness, the OH concentration was held constant, although, in reality, it increased under polluted conditions (Fig. 1*A*). Fig. 3*A* shows the simulated dependence of $f_{\mathrm{HO_2}}$, f_{NO}, $f_{\mathrm{RO_2}}$, and f_{ISOM} on NO concentration. Under polluted conditions of greater than several hundred ppt of NO, ISOPOO loss is dominated by reaction with NO (e.g., 90% for 400 ppt NO). Under less polluted conditions, the other three reaction pathways become important.

Fig. 3*B* shows the simulated dependence of production ratio χ on NO concentration and allows an inference of an effective NO concentration associated with the confidence interval 0.6–0.9 for χ. As a point of reference, background NO mixing ratios of 15–60 ppt (36), 10–30 ppt (37), 20–80 ppt (31), and 35 ppt (mean value of GoAmazon2014/5 aircraft measurement; *SI Appendix*, Fig. S5) have been measured for the central region of the Amazon basin for studies from 1985 through 2014. These ranges are represented by the brown arrows in Fig. 3*B*. According to Fig. 3*B*, the effective NO concentration associated with the confidence interval of χ ranged from 16 to 30 ppt (Fig. 3, yellow shading). This effective value represents the net chemistry across the history of the air parcel. The good agreement between the effective NO concentration inferred in this way and the range of measured ambient concentrations for background conditions lends confidence to the accuracy of the overall model framework of the present study. Across the range of effective NO concentrations, the following fractional contributions to ISOPOO reaction are obtained: $0.31 < f_{\mathrm{HO_2}} < 0.39$, $0.27 < f_{\mathrm{NO}} < 0.40$, $0.03 < f_{\mathrm{RO_2}} < 0.05$, and $0.25 < f_{\mathrm{ISOM}} < 0.30$ (Fig. 3*A*, yellow

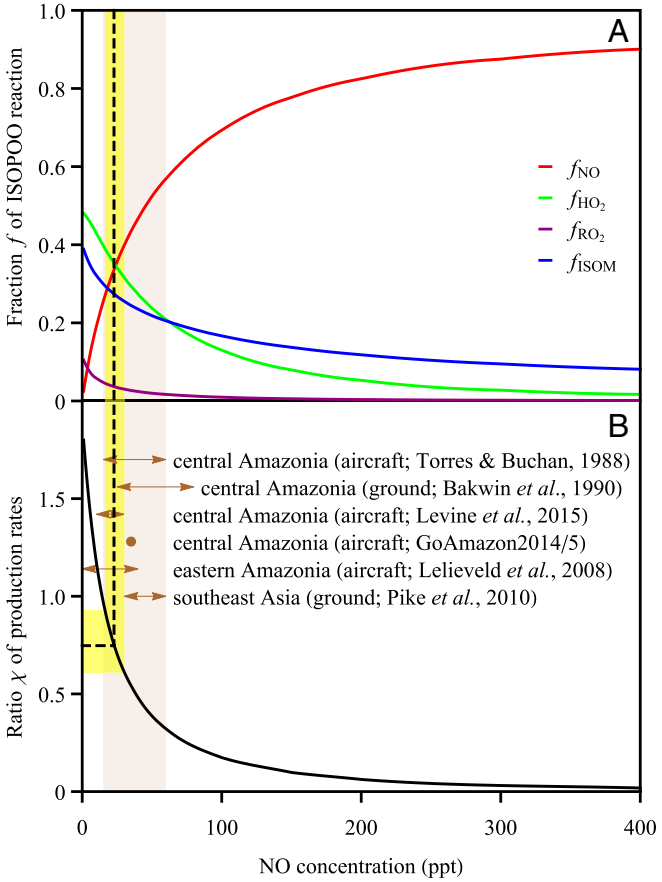

Fig. 3. Modeled dependence on NO concentration of (*A*) fractional contributions f_{HO_2}, f_{NO}, f_{RO_2}, and f_{ISOM} to ISOPOO reactive loss and (*B*) the ratio χ of the production rate of ISOPOOH to that of MVK + MACR. The brown arrows represent the reported ranges of NO concentration for central Amazonia, eastern Amazonia, and southeast Asia under background conditions (2, 31, 36, 37, 48). The gray region represents NO concentrations reported by Torres and Buchan (36) for measurements in 1985. The dashed line projects the central value of χ for background conditions onto the effective NO concentration, illustrating the possible relative contributions of different reaction pathways of ISOPOO. The yellow region shows the same as the dashed line but for confidence interval in χ.

shading). Notably, compared with the wide range of NO concentrations reported (Fig. 3*A*, gray shading), the effective NO concentrations based on our observation provide a tighter constraint to ISOPOO reaction under background conditions. Specifically, the confidence interval of the f_{HO_2}-to-f_{NO} ratio spans 0.8–1.4. This result is robust with respect to the inclusion or not of the isomerization pathway (*SI Appendix*, Table S3). An important point to emphasize is that the modeling analysis leading to this ratio for background conditions is ultimately constrained by the measured concentrations of ISOPOOH, MVK + MACR, and NO_y.

Implications

The ranges in f_{NO}, f_{HO_2}, f_{RO_2}, and f_{ISOM} for the yellow region of Fig. 3*A* imply that the HO_2 pathway accounted for 31–39% of the reactive loss of ISOPOO under the low-NO conditions of the wet season in the central Amazon basin. Conversely, reactions with NO under low-NO conditions accounted for 27–40% of ISOPOO loss. For comparison with these values, a state-of-the-art CTM predicted that the HO_2 pathway contributed 59% of the reactive loss of ISOPOO radicals for the grid box of 4° × 5° encompassing the measurement site and that the contribution of the NO pathway to reactive loss was 14% for a typical wet season (*SI Appendix*, Table S4). An overestimate in models of the importance of the HO_2 pathway for ISOPOO reactive loss has important implications for predicted concentrations of organic particulate matter (5) and consequent connections among flora, oxidative capacity, aerosol particles, cloud condensation nuclei, clouds, and rainfall over this vast tropical forest (38). An underestimate of the NO pathway in central Amazonia can have profound impacts on the predicted concentrations of isoprene nitrates transported to adjacent regions, influencing NO_x concentrations and photochemistry in those regions (39). In addition, given the importance of this geographical region in the global isoprene budget (1), previous estimates of the fraction of ISOPOO reacting via the HO_2 pathway on a global basis by CTMs might also be too high (10). Future studies are needed to better constrain the fraction of ISOPOO reactive loss via the HO_2 pathway in other locations having high isoprene concentrations and low anthropogenic NO_x emissions.

One possible reason, among others, for the gap between observations and the CTM model predictions is an underprediction of NO concentrations and hence an underestimate of the importance of the NO reaction pathway in the model. The modeled daytime average concentration of NO was 8 ppt for the grid box in which the measurement site was located. This value is much lower than the range of NO concentrations measured in central Amazonia (Fig. 3). Furthermore, the modeled daytime concentration of NO_y was 0.1 ppb, which is 80% lower than the observed background NO_y concentrations in central Amazonia (31). Underpredicted NO and NO_y concentrations in the model might, in turn, be related to underestimated NO emissions from tropical forests. Flux measurements have shown that soils have high emissions of NO_x in the forested regions of both central Amazonia (40–43) and southeast Asia (44). The above-soil NO_x emission modeled in the CTM for the wet season of central Amazonia was 10 times lower than the observations reported in the literature (*SI Appendix*). Ganzeveld et al. (45) additionally suggest that CTMs might underestimate the fraction of soil-emitted NO_x that survives transport through tropical forest layers and is ultimately emitted to the overlying atmosphere. Herein, additional model runs were performed as a sensitivity study to establish that increasing NO_x emissions above canopy by a factor of 30 can bring the modeled ratio ξ closer to its observed range (*SI Appendix*). Any change made to model emissions on this basis must, however, also assess possible perturbations of other modeled quantities, such as ozone or hydroxyl radical concentrations, compared with measured values (2, 46).

In outlook, current trends in human activities, including ongoing land use changes for agricultural activities as well as growing urbanization, are associated with the continual reduction of forest coverage in the Amazon basin (47). These trends, in turn, lead to increased demand for electricity and transport, which, with current technologies, increases NO_x emissions (44). With respect to the atmospheric chemistry of the region, the concentration ratio ξ and its complement of the production ratio χ serve as surrogates of the qualitative characteristics of isoprene chemistry, with associated effects that are of concern to humans, such as production of ozone and organic particulate matter and changes in visibility and rainfall, among others (3, 38). Under background conditions, expressed as 75% confidence intervals, the ratio of the fractional contribution by HO_2 to the reactive loss of ISOPOO to that by NO ranges from 0.8 to 1.4, the ratio of the production rate χ of ISOPOOH to that of MVK + MACR ranges from 0.6 to 0.9, and the ratio ξ of the concentration of ISOPOOH to that of MVK + MACR ranges from 0.4 to 0.6. In this regard, the data (Fig. 2, ξ) and the model (Fig. 3, χ) show that the oxidant cycle is highly sensitive to changes from background to polluted conditions. The implication is that small increases in NO concentration above the background level can lead to a large change in the aforementioned endpoints of air quality and climate. In particular, the abrupt drop in ISOPOOH concentration associated with pollution speaks to the extent of

human-induced changes in photochemical cycles over the rain forest, both at present during times of widespread biomass burning in the dry season and, possibly, in the future during all seasons as a consequence of economic development and increasing pollution throughout the Amazon basin.

Materials and Methods

Measurements were made at the T3 site of the GoAmazon2014/5 Experiment (25). A PTR-TOF-MS (Ionicon Analytik) equipped with a cold trap was used to measure ISOPOOH and MVK + MACR concentrations. The approach was to collect data for a period with the trap in line to quantify MVK+MACR followed by a period in bypass to quantify MVK+MACR+ISOPOOH. Detailed additional information about the measurements and associated modeling is provided in *SI Appendix*.

ACKNOWLEDGMENTS. We thank John Crounse and Paul Wennberg for supporting GEOS-Chem simulations. We thank Ronald Cohen and Yi Li for helpful discussions. Institutional support was provided by the Central Office of the Large Scale Biosphere Atmosphere Experiment in Amazonia (LBA), the National Institute of Amazonian Research (INPA), and Amazonas State University (UEA). We acknowledge the Atmospheric Radiation Measurement (ARM) Climate Research Facility, a user facility of the United States Department of Energy, Office of Science, sponsored by the Office of Biological and Environmental Research, and support from the Atmospheric System Research (ASR) program of that office. Funding was obtained from the United States Department of Energy (DOE), the Amazonas State Research Foundation (FAPEAM), the São Paulo Research Foundation (FAPESP), the Brazilian Scientific Mobility Program (CsF/CAPES), and the United States National Science Foundation (NSF). The research was conducted under Scientific License 001030/2012-4 of the Brazilian National Council for Scientific and Technological Development (CNPq).

1. Guenther A, et al. (2012) The Model of Emissions of Gases and Aerosols from Nature version 2.1 (MEGAN2.1): An extended and updated framework for modeling biogenic emissions. *Geosci Model Dev* 5(6):1471–1492.
2. Lelieveld J, et al. (2008) Atmospheric oxidation capacity sustained by a tropical forest. *Nature* 452(7188):737–740.
3. Chameides WL, Lindsay RW, Richardson J, Kiang CS (1988) The role of biogenic hydrocarbons in urban photochemical smog: Atlanta as a case study. *Science* 241(4872):1473–1475.
4. Claeys M, et al. (2004) Formation of secondary organic aerosols through photooxidation of isoprene. *Science* 303(5661):1173–1176.
5. Paulot F, et al. (2009) Unexpected epoxide formation in the gas-phase photooxidation of isoprene. *Science* 325(5941):730–733.
6. Surratt JD, et al. (2010) Reactive intermediates revealed in secondary organic aerosol formation from isoprene. *Proc Natl Acad Sci USA* 107(15):6640–6645.
7. Karl T, et al. (2007) The tropical forest and fire emissions experiment: Emission, chemistry, and transport of biogenic volatile organic compounds in the lower atmosphere over Amazonia. *J Geophys Res* 112(D18):D18302.
8. Kuhn U, et al. (2007) Isoprene and monoterpene fluxes from Central Amazonian rainforest inferred from tower-based and airborne measurements, and implications on the atmospheric chemistry and the local carbon budget. *Atmos Chem Phys* 7(11):2855–2879.
9. Jenkin ME, Young JC, Rickard AR (2015) The MCM v3.3.1 degradation scheme for isoprene. *Atmos Chem Phys* 15(20):11433–11459.
10. Crounse JD, Paulot F, Kjaergaard HG, Wennberg PO (2011) Peroxy radical isomerization in the oxidation of isoprene. *Phys Chem Chem Phys* 13(30):13607–13613.
11. Liu YJ, Herdlinger-Blatt I, McKinney KA, Martin ST (2013) Production of methyl vinyl ketone and methacrolein via the hydroperoxyl pathway of isoprene oxidation. *Atmos Chem Phys* 13(11):5715–5730.
12. Chen Q, et al. (2015) Submicron particle mass concentrations and sources in the Amazonian wet season (AMAZE-08). *Atmos Chem Phys* 15(7):3687–3701.
13. Rivera-Rios JC, et al. (2014) Conversion of hydroperoxides to carbonyls in field and laboratory instrumentation: Observational bias in diagnosing pristine versus anthropogenically-controlled atmospheric chemistry. *Geophys Res Lett* 41(23):8645–8651.
14. Jenkin ME, Boyd AA, Lesclaux R (1998) Peroxy radical kinetics resulting from the OH-initiated oxidation of 1,3-butadiene, 2,3-dimethyl-1,3-butadiene and isoprene. *J Atmos Chem* 29(3):267–298.
15. Peeters J, Müller J-F, Stavrakou T, Nguyen VS (2014) Hydroxyl radical recycling in isoprene oxidation driven by hydrogen bonding and hydrogen tunneling: The upgraded LIM1 mechanism. *J Phys Chem A* 118(38):8625–8643.
16. Fuchs H, et al. (2011) Detection of HO_2 by laser-induced fluorescence: Calibration and interferences from RO_2 radicals. *Atmos Meas Tech* 4(6):1209–1225.
17. Hoell JM, et al. (1987) Airborne intercomparison of nitric oxide measurement techniques. *J Geophys Res* 92(D2):1995–2008.
18. Hewitt CN, et al. (2010) Overview: oxidant and particle photochemical processes above a south-east Asian tropical rainforest (the OP3 project): Introduction, rationale, location characteristics and tools. *Atmos Chem Phys* 10(1):169–199.
19. Wennberg PO (2013) Let's abandon the "high NO_x" and "low NO_x" terminology. *IGAC News* 50:3–4.
20. Perring AE, Pusede SE, Cohen RC (2013) An observational perspective on the atmospheric impacts of alkyl and multifunctional nitrates on ozone and secondary organic aerosol. *Chem Rev* 113(8):5848–5870.
21. de Gouw J, Warneke C (2007) Measurements of volatile organic compounds in the Earth's atmosphere using proton-transfer-reaction mass spectrometry. *Mass Spectrom Rev* 26(2):223–257.
22. Karl T, et al. (2009) Rapid formation of isoprene photo-oxidation products observed in Amazonia. *Atmos Chem Phys* 9(20):7753–7767.
23. Worton DR, et al. (2013) Observational insights into aerosol formation from isoprene. *Environ Sci Technol* 47(20):11403–11413.
24. Xiong F, et al. (2015) Observation of isoprene hydroxynitrates in the southeastern United States and implications for the fate of NO_x. *Atmos Chem Phys* 15(19):11257–11272.
25. Martin ST, et al. (2016) Introduction: Observations and Modeling of the Green Ocean Amazon (GoAmazon2014/5). *Atmos Chem Phys* 16(8):4785–4797.
26. Nguyen TB, et al. (2015) Rapid deposition of oxidized biogenic compounds to a temperate forest. *Proc Natl Acad Sci USA* 112(5):E392–E401.
27. Karl T, et al. (2013) Airborne flux measurements of BVOCs above Californian oak forests: Experimental investigation of surface and entrainment fluxes, OH densities, and Damköhler numbers. *J Atmos Sci* 70(10):3277–3287.
28. Chen Q, et al. (2009) Mass spectral characterization of submicron biogenic organic particles in the Amazon Basin. *Geophys Res Lett* 36(20):L20806.
29. Martin ST, et al. (2010) Sources and properties of Amazonian aerosol particles. *Rev Geophys* 48(2):RG2002.
30. Nguyen TB, et al. (2014) Overview of the Focused Isoprene eXperiment at the California Institute of Technology (FIXCIT): Mechanistic chamber studies on the oxidation of biogenic compounds. *Atmos Chem Phys* 14(24):13531–13549.
31. Bakwin PS, Wofsy SC, Fan S-M (1990) Measurements of reactive nitrogen oxides (NO_y) within and above a tropical forest canopy in the wet season. *J Geophys Res* 95(D10): 16765–16772.
32. Valin LC, Russell AR, Cohen RC (2013) Variations of OH radical in an urban plume inferred from NO_2 column measurements. *Geophys Res Lett* 40(9):1856–1860.
33. Kim S, et al. (2013) Evaluation of HO_x sources and cycling using measurement-constrained model calculations in a 2-methyl-3-butene-2-ol (MBO) and monoterpene (MT) dominated ecosystem. *Atmos Chem Phys* 13(4):2031–2044.
34. Vilà-Guerau de Arellano J, van den Dries K, Pino D (2009) On inferring isoprene emission surface flux from atmospheric boundary layer concentration measurements. *Atmos Chem Phys* 9(11):3629–3640.
35. St Clair JM, et al. (2016) Kinetics and products of the reaction of the first-generation isoprene hydroxy hydroperoxide (ISOPOOH) with OH. *J Phys Chem A* 120(9):1441–1451.
36. Torres AL, Buchan H (1988) Tropospheric nitric oxide measurements over the Amazon Basin. *J Geophys Res* 93(D2):1396–1406.
37. Levine JG, et al. (2015) Isoprene chemistry in pristine and polluted Amazon environments: Eulerian and Lagrangian model frameworks and the strong bearing they have on our understanding of surface ozone and predictions of rainforest exposure to this priority pollutant. *Atmos Chem Phys Discuss* 15(17):24251–24310.
38. Pöschl U, et al. (2010) Rainforest aerosols as biogenic nuclei of clouds and precipitation in the Amazon. *Science* 329(5998):1513–1516.
39. Ito A, Sillman S, Penner JE (2007) Effects of additional nonmethane volatile organic compounds, organic nitrates, and direct emissions of oxygenated organic species on global tropospheric chemistry. *J Geophys Res* 112(D6):D06309.
40. Bakwin PS, et al. (1990) Emission of nitric oxide (NO) from tropical forest soils and exchange of NO between the forest canopy and atmospheric boundary layers. *J Geophys Res* 95(D10):16755–16764.
41. Verchot LV, et al. (1999) Land use change and biogeochemical controls of nitrogen oxide emissions from soils in eastern Amazonia. *Global Biogeochem Cycles* 13(1):31–46.
42. Garcia-Montiel DC, et al. (2001) Controls on soil nitrogen oxide emissions from forest and pastures in the Brazilian Amazon. *Global Biogeochem Cycles* 15(4):1021–1030.
43. Kaplan WA, Wofsy SC, Keller M, Da Costa JM (1988) Emission of NO and deposition of O_3 in a tropical forest system. *J Geophys Res* 93(D2):1389–1395.
44. Hewitt CN, et al. (2009) Nitrogen management is essential to prevent tropical oil palm plantations from causing ground-level ozone pollution. *Proc Natl Acad Sci USA* 106(44):18447–18451.
45. Ganzeveld LN, et al. (2002) Global soil-biogenic NO_x emissions and the role of canopy processes. J Geophys Res 107(D16):4298.
46. Jacob DJ, Wofsy SC (1988) Photochemistry of biogenic emissions over the Amazon forest. *J Geophys Res* 93(D2):1477–1486.
47. Davidson EA, et al. (2012) The Amazon basin in transition. *Nature* 481(7381):321–328.
48. Pike RC, et al. (2010) NO_x and O_3 above a tropical rainforest: An analysis with a global and box model. *Atmos Chem Phys* 10(21):10607–10620.